SSRG International Journal of Civil Engineering
ISSN: 2348-8352/ https://doi.org/10.14445/23488352/IJCE-V13I8P132

Volume 13 Issue 8, 560-578, August 2026

Original Article

Reliability-Based Evaluation of Long-Term Deflection in Reinforced Concrete Flanged Beams: A Unified FOSM-Monte Carlo Simulation Framework with Dual Sensitivity Analysis and Design Implications

Madhusudhan M S[1], Umesha P K[2]

[1,2]*Department of Civil Engineering, Vidyavardhaka College of Engineering, Karnataka, India.*

[1]*Corresponding Author : madhushivaprakash@gmail.com*

Received: 08 May 2026 Revised: 22 July 2026 Accepted: 18 August 2026 Published: 31 August 2026

Abstract *- The potential for long-term deflection to govern the serviceability of flanged beams results from the combined effects of the sustained loading on the beams, as well as factors like cracking, creep, and shrinkage that contribute to the reduction of the margin between calculated and prescribed deflection limits. While deterministically determining the deflection of beams ensures that the deflection specification is satisfied, no information is obtained regarding the probability that the beam will experience deflection that reaches the prescribed limit state. Eight flanged beams of various section depths were evaluated, each with a span length of 5,000 mm. For each beam, the total deflection limit of l/250, or 20 mm as prescribed in the Indian standard code IS 456:2000 was utilized to define the serviceability limit state. Additionally, the limit state can be defined in terms of the individual components of deflection: instantaneous, shrinkage, and creep. Eighteen structural and material variable characteristics were determined for each of the eight beams. For the reliability analysis, eight of the variables were utilized: the sustained bending moment, the span length, the elastic modulus of the concrete, the effective moment of inertia, the shrinkage curvature of the beam, the modulus of elasticity of the concrete that has been creep-modified, the long-term effective moment of inertia, and the moment that is applied to the beam under the sustained load. The reliability of each beam was calculated using the First Order Second Moment (FOSM) method, as well as Monte Carlo simulation utilizing 100,000 samples to determine the reliability of each beam. Furthermore, methods were utilized to determine the local sensitivity of the beams, including analyzing the inclusion of variables, the suppression of individual variables, and the importance of the variance of each variable. Results of the analysis indicate that as the tabulated depth of each beam decreases from 450 mm to 310 mm, the mean total deflection of each beam increases from 10.464 mm to 16.982 mm, or an increase of 62.3%. Additionally, the reliability of each beam calculated via FOSM indicates that as depth decreases, the FOSM reliability index decreases from 4.634 to 1.018, with the corresponding failure probabilities increasing from 1.79×10^{-6} to 1.54×10^{-1}. Monte Carlo method results indicate that the mean total deflection of each beam increases from 10.547 mm to 17.131 mm, an increase of 62.4%, and that the failure probability increases from 5.00×10^{-5} to 1.37×10^{-1}, with reliability indices of 3.891 and 1.094, respectively. Comparison of the two methods indicates that the FOSM approximation is non-conservative for the deeper sections, returning a reliability index 19.1% above the simulated value at a depth of 450 mm, and mildly conservative for the shallowest sections, returning a value 6.9% below the simulated one at a depth of 310 mm, the sign of the deviation changing at an effective depth of approximately 340 mm. Additionally, each of the variables related to the sustained load on the beams contributed to approximately 60.3% to 65.8% of the total deflection of each beam. Furthermore, analysis of each of the eight beams indicates that the shallowest depth of 410 mm is the shallowest depth of any of the beams studied at which each method achieved a reliability index of 3.0 or more; thus, the depth-to-reliability relationship is only preliminary and should be applied to beams of the same span length, similar material properties, similar support conditions, and with a sustained load of 40%. A more thorough application of these methods to other beams would require additional experimental validation of the results.*

Keywords *- First-Order Second-Moment method, IS 456:2000, Long-term deflection, Monte Carlo simulation, Probabilistic design, Reinforced concrete flanged beams, Reliability index.*

1. Introduction

The deflection performance of beams that are in-service and experience loading over time is a topic that has been covered in the codes of practice that are currently in use in most of the world. The deflection of beams under load over time can be the result of the initial elastic deflection of the beam under the applied load, the additional deflection due to shrinkage, and the additional deflection due to the creep of the beams' materials over time; the total deflection of the beam over time can, therefore, be up to twice the initial deflection measurement of the beam under static loading. Beams that have flanges, such as T-section beams and L-section beams, are common in construction projects. The flange of these beams can experience different shrinkage rates to the remainder of the beam; the different shrinkage of the flange and the beam's web creates different behaviours for flanged beams compared to beams with rectangular cross-sections.

The deterministic approach to meeting the serviceability limit of deflection in the code IS 456:2000 Clause 23.2 limits the total long-term deflection of beams to a fraction of l/250, and limits the deflection that develops after the installation of partitions within the beams to a fraction of l/350 or 20 mm, whichever value is smaller. These limits were established empirically and have implicit safety factors associated with them; these factors are not visible to the designer within the deterministic equations, however. Two beams that have the same deterministically calculated deflection may have very different probabilities of failure; no such assurance is made within the code.

A probabilistic approach to reliability theory makes it possible to calculate the probability that the limit state function of the beams is violated. The First Order Second-Moment method can be used to provide a relatively-easy calculation of this probability, as well as understand the contribution of each of the random variables to the total deflection of the beams. Monte Carlo simulation methods can be used to cross-validate the accuracy of these calculations. Additionally, a comparison between the results of the First-Order Second-Moment method calculations and Monte Carlo simulation calculations can indicate the degree of nonlinearity of the limit state function.

The serviceability of reinforced concrete beams under long-term loading is governed by the coupled uncertainties of loading, span, stiffness of the cracked section, and creep and shrinkage deformations. The determination of the deflection ratio for a beam under service loads only tells a designer whether the deflection is within some limit; it tells nothing of the probability that the beam will deflect to an amount that is beyond that limit. Thus, two beams with similar ratios of loading to allowable loading may have vastly different reliability characteristics. The literature on reliability of beam deflection is limited to studies that provide no external validation of their results, examine the complete long-term deflection of beams, or compare the various parameters that influence that deflection.

The literature on the subject of long-term serviceability of reinforced concrete beams primarily addresses the separate elements of the problem. Abdel-Hafez investigated the reliability of code-based equations for calculating short-term deflections. Patil and Manjunath investigated the nonuniform reliability of flanged beams, extending their study to incorporate time-dependent deflection due to creep and shrinkage. Other investigations into the subject of long-term deflection included studies on nonlinear creep and shrinkage in deep beams, environmental deterioration of beams strengthened with carbon-fiber-reinforced polymers, experimental investigations of time-dependent deflection, and global sensitivity analyses of long-term deflection of beams. Nevertheless, none of these investigations simultaneously consider the aspects of establishing a limit state for long-term deflection of flanged beams, performing a FOSM analysis that accounts for the covariance of the input variables, performing Monte Carlo simulations to estimate the reliability of flanged beams, performing both local and global sensitivity analyses of the variables that impact the reliability of flanged beams, performing independent validation of these analyses, performing reliability assessments according to different building codes, and performing inverse design of beams according to a desired reliability. Thus, the identified need in the field is not for the introduction of any of these individual methods, but for their integration into a framework that connects these concepts and allows for the assessment of the reliability of flanged beams according to the provisions of building codes.

Research gap and problem statement. Three specific deficiencies emerge from the foregoing survey. First, existing reliability studies of RC beam deflection treat either the instantaneous component in isolation (Abdel-Hafez, 2006) or the time-dependent component with a deterministic creep coefficient (Patil and Manjunath, 2011), so that the joint uncertainty of the instantaneous, shrinkage and creep contributions has never been propagated through a single limit-state function written in the form prescribed by IS 456:2000. Second, where Monte Carlo simulation has been applied to long-term deflection (Beheshti Aval and Ghabdian, 2019; Ghabdian et al., 2022; Guo et al., 2025), the members analysed are deep beams, general flexural members or FRP-reinforced sections rather than conventional flanged beams, and the reported reliability indices are seldom accompanied by the sampling error that governs their credibility in the rare-event region. Third, the local sensitivity structure of the long-term deflection limit state, that is, which of the code-defined random variables actually controls the reliability index, has not been quantified for flanged beams, with the consequence that a designer who finds a section deficient has no guidance on which parameter to tighten. The problem addressed in this paper follows directly from these three deficiencies: given a family of flanged beams that all satisfy the deterministic deflection provisions of IS 456:2000, how wide is the spread in their actual serviceability reliability, which variables generate that spread, and at what slenderness does the reliability index fall below the target value adopted for serviceability limit states?

The novelty of the investigation is not derived from the use of FOSM, Monte Carlo simulation and global sensitivity analysis methods individually, all of which are well established in the context of structural reliability. Instead, the main contribution of the present investigation is the application of these methods to the assessment of the long-term serviceability of RC flanged beams. The proposed methodology includes the formulation of a limit state function that accounts for instantaneous, shrinkage and creep deflections; the application of first-order reliability method that uses both FOSM and Monte Carlo simulations to compute the reliability index with confidence intervals; local sensitivity analysis alongside Sobol first and total order sensitivity indices to determine the impact of nonlinear effects; the use of experimental deflection measurements to validate the proposed reliability indices; a comparison of the reliability indices predicted by IS 456, ACI and Eurocode codes; and the determination of the depth or slenderness of the beams that would ensure the target reliability indices are achieved. All of these analyses can be performed simultaneously on a set of beams with different design and geometrical parameters to assess the compliance of these beams with deterministic and probabilistic design requirements.

The present study develops a framework for evaluating serviceability and reliability of reinforced concrete flanged beams by combining: (i) a limit-state function that includes the instantaneous, shrinkage-induced and creep-induced deflections; (ii) estimates of the structural reliability based on both first-order reliability method and Monte Carlo simulations for eight different beam configurations; (iii) local sensitivity analyses based on both variable inclusion and variable suppression methods, in addition to first-order reliability method-based measures of variance importance; and (iv) the translation of these results into a preliminary design chart. The major contribution of this study, therefore, is the combination of these four components for evaluating long-term deflection, reliability, local sensitivity and reliability-based sizing for beams within the scope of the investigated code standard. The use of experimental testing, Sobol sensitivity analyses, or other analyses that evaluate reliability within codes other than IS 456 are considered necessary extensions of the current study, but are not the major contributions to the field of reinforced concrete design that are made by the current investigation.

2. Literature Review

2.1. Time-Dependent Deflection in RC Beams

The concept of long-term deflection in Reinforced Concrete (RC) beams is based on the understanding of elastic analyses of beams, such as those based on ACI 318 or IS 456:2000. These analyses consider the elastic deflection of beams subjected to bending moments and do not consider the effects of time-dependent variables such as creep and shrinkage. More sophisticated analyses, however, have attempted to include in their calculations variables associated with the long-term behavior of RC beams. Gilbert and Warner (1978) were among the first to provide an analysis of the effects of tension stiffening in beams subjected to flexure, leading to the concept of effective moment of inertia, incorporated into codes such as IS 456:2000 and ACI 318. Charkas et al. (2002) published a study on the load-deflection behavior of FRP-strengthened beams, demonstrating how the loading history of those beams could be incorporated into the calculations of their deflections. Abdel-hafez (2006) provided a study of the reliability of the deflection equations within the IS 456:2000 code for beams, finding that the short-term deflections predicted by the code had reliability of β values of between 2.5 and 4.0. These studies are the foundation upon which the long-term deflection of RC beams can be analyzed using probabilistic methods.

Section geometry and reinforcement type condition the time-dependent response as strongly as the material model. Al-Ansari (2015) analysed the reliability and flexural behaviour of triangular and T-shaped reinforced concrete beams and showed that a non-rectangular compression zone alters both the mean resistance and its dispersion relative to an equivalent rectangular section, which is the principal reason that reliability results derived for rectangular beams cannot be transferred to flanged beams without recalculation. Hawileh et al. (2022) quantified the influence of flange geometry on the behaviour of RC T-beams and confirmed that the flange contributes disproportionately to the stiffness terms that enter the effective moment of inertia, so that the flange width and thickness must be carried explicitly into any stochastic model of Ieff. For non-conventional reinforcement, Ali (2014) evaluated the time-dependent reliability of FRP-strengthened beams under coupled corrosion and changing load, and Feng et al. (2022) developed reliability-based design recommendations for FRP-reinforced compression-yield beams using Monte Carlo simulation. Both studies concluded that the serviceability limit state, rather than the ultimate limit state, governs members whose reinforcement has a low elastic modulus, which is precisely the condition that a long-span flanged beam approaches as its depth is reduced.

2.2. Reliability Methods Applied to RC Beams

The formulation of first-order reliability methods (FOSM) was established by Lind (1971) and Hasofer and Lind (1974). Since their publication, FOSM methods have been applied to a variety of limit states within RC beams. For instance, Pustka (2014) performed a reliability analysis of high-performance beams based on FOSM methods, finding that the strength limit state is insensitive to the coefficient of variation (COV) of the load assumptions for COVs below 0.10, but that the strength limit state becomes increasingly sensitive to the COV of the load distribution for higher COVs - a factor that is relevant to the analysis of beams under sustained moments, whose COV is around 0.15. Patil and Manjunath (2010) published an equation for the reliability index, β, for flanged beams at the deflection limit state.

Subsequent work by the same authors (2011) applied the reliability methods to time-dependent variables, such as creep, however only in a deterministic method for estimating the creep coefficient. Firouzi et al. (2019) published a study on the reliability of beams strengthened with CFRP under environmental deterioration effects, allowing for deterioration variables to be included in Monte Carlo Simulations (MCS) methods of reliability analyses.

The computational treatment of the reliability integral has developed in parallel with these applications. Kaliszuk (2011) demonstrated that hybrid Monte Carlo schemes, in which an approximation of the limit state replaces repeated structural analysis, reduce the sample count required for a stable failure-probability estimate by more than an order of magnitude, and set out the sampling-error expression that governs the credibility of any simulated failure probability in the rare-event region. Grubišić et al. (2019) applied finite element based reliability analysis to reinforced concrete frames with implicit limit state functions and showed that the first-order approximation degrades appreciably once the reliability index exceeds approximately 3.5, a threshold that proves directly relevant to the serviceability calculations reported in Section 5.2 of the present work. At the level of design philosophy, Wen (2001) formalised the relationship between target reliability indices and performance-based acceptance criteria, and it is this framework that allows a serviceability target such as a reliability index of 3.0 to be treated as an explicit design constraint rather than as a post-hoc check.

More recent work has extended time-dependent reliability analysis to progressively more refined material models. Beheshti Aval and Ghabdian (2019) coupled an adaptive neuro-fuzzy inference surrogate with Monte Carlo simulation to evaluate the time-dependent reliability of RC deep beams under linear and nonlinear creep and shrinkage, validating the underlying finite element model against short- and long-term beam tests. Ghabdian et al. (2022) subsequently generalised microprestress-solidification creep theory to treat creep, shrinkage and elevated temperature simultaneously within a serviceability reliability framework intended for structural health monitoring. Dan et al. (2023) replaced the mechanical model altogether with polynomial-chaos, support-vector, Kriging and radial-basis surrogates for the long-term deflection of RC flexural members, and used the polynomial chaos expansion to obtain global sensitivity indices, concluding that geometric parameters influence long-term deflection more strongly than material parameters. Guo et al. (2025) developed a layered section model for the long-term deflection of FRP-reinforced compression-yield beams and assessed the serviceability limit state by Monte Carlo simulation, reporting that the rate of reliability degradation over the service life is sensitive to the creep model adopted. These four studies establish the maturity of simulation-based serviceability reliability analysis; each of them, however, is directed at a member type, namely deep beams, general flexural members or FRP-reinforced sections, that lies outside the class of conventional RC flanged beams designed to IS 456:2000, and none of them reports the local sensitivity of the reliability index to the individual code-defined variables.

2.3. Comparative Synthesis and Research Gap

Despite the various developments in the reliability analyses for RC beams described above, no studies have yet undertaken an investigation that includes each of the four elements described in this paper. Each of these elements relates to the long-term deflection of beams using the complete formulation of IS 456:2000 code provisions, treating each of the variables associated with that code as stochastic variables.

Furthermore, the study should investigate the sensitivity of the variables of interest, both by adding each variable to the model, and suppressing each of those variables; additionally, validation of FOSM methods against MCS methods should occur. Finally, there should be an output of results that can be applied to the practice of beam design. The present study aims to address each of these elements for flanged beams of varying depths, between L/D ratios of 12 and 18.

2.4. Novelty of the Present Study

Table 1 compares the present approach to the papers most closely related to deflection reliability, time-dependent concrete behaviour and uncertainty analysis. The comparison distinguishes between the structural element studied, treatment of creep and shrinkage, reliability analysis approach, validation, global sensitivity analysis and the transfer of results to code- or design- provisions. The aim of the comparison is to reveal the methodological gap as a whole rather than to suggest that the individual approaches used in the present study are new.

The comparative synthesis of the above literature reveals that each of the components of the current study has been investigated in isolation in the past. Studies on flanged beams have investigated the reliability of deflection in beams over time using Monte Carlo simulation methods. More recent investigations into creep and deterioration have used nonlinear models for creep, performed experiments to validate the results of the creep models, investigated the effects of environmental deterioration of beams, surrogate modelling methods and global sensitivity analysis; however, the majority of these investigations have used deep beams, beams with added reinforcement, general beams, or other systems beyond conventional reinforced concrete flanged beams. Thus, the novelty of this study is not in the application of FOSM, MCS, creep models, or Sobol sensitivity indices methods individually; rather, the novelty of this study lies in the integration of these methods into a reliability analysis of conventional reinforced concrete flanged beams developed for long-term deflection analysis of such beams.

Table 1. Comparison of representative studies on probabilistic and long-term deflection assessment of reinforced concrete beams

Study	Flanged beam	Long-term creep/ shrinkage	FOSM	MCS	External validation	Global sensitivity	Code/design output
Abdel-Hafez (2006)	No	No—short-term deflection	NR	NR	NR	No	Partial—assessment of code deflection equations
Patil and Manjunath (2010)	Yes	No	NR	No/NR	No	No	Yes—empirical reliability expression and depth selection
Patil and Manjunath (2011)	Yes	Yes	No/ NR	Yes	No	No	Partial—IS 456-oriented time-dependent design implications
Beheshti Aval and Ghabdian (2019)	No—deep and shallow beams	Yes, including nonlinear creep	No	Yes	Yes—FEM checked against experimental results	No	Partial—serviceability and strength recommendations
Firouzi et al. (2019)	Not specifically	No—environmental deterioration and corrosion instead	No	No—first-passage reliability	No independent deflection validation	No	Partial—FRP/code-oriented reliability implications
Ghabdian et al. (2022)	No	Yes, including temperature and cracking	No	Yes	Yes—published and author-generated experiments	No	Partial—serviceability reliability findings
Dan et al. (2023)	No—general RC flexural members	Yes	No	No—surrogate modelling	Yes—numerical and experimental datasets	Yes	Limited—prediction and uncertainty interpretation
Guo et al. (2025)	No—FRP RC beams	Yes	No	Yes	Model-oriented comparison	No	Partial—serviceability reliability comparison
Present study	Yes	Yes	Yes	Yes—N = 100,000, with sampling error and 95% confidence intervals	No—cross-verified against MCS; experimental validation identified as future work	No—local sensitivity by variable inclusion, variable suppression and variance importance	Yes—preliminary IS 456 depth/slenderness design chart

Quantitative positioning against previous findings. The reliability levels obtained here can be compared directly with values already in the literature. Abdel-Hafez (2006) reported a reliability index between 2.5 and 4.0 for the short-term deflection limit state of code-designed members; the present analysis returns 4.634 at a slenderness of 12 but only 1.018 at a slenderness of 18.2 once shrinkage and creep are admitted as random variables, which shows that a short-term assessment overstates the available margin in a slender flanged beam by a factor of between 2.5 and 3.9. Patil and Manjunath (2010, 2011) established that flanged beams designed to a common deflection provision do not possess uniform reliability, but did not quantify the rate of decay; the present results give that decay explicitly as a loss of approximately 0.58 units of reliability index per unit increase in the span-to-depth ratio over the range from 12 to 18.2. Beheshti Aval and Ghabdian (2019) and Ghabdian et al. (2022) obtained comparable orders of failure probability for deep beams and for serviceability governed by microprestress-solidification creep, but their frameworks require a finite element model or a trained surrogate, whereas the closed-form limit state adopted here reproduces the simulated reliability index to within 2.4% in the range from 2.0 to 2.1 at approximately four orders of magnitude fewer model evaluations. Dan et al. (2023) concluded from a global sensitivity analysis of surrogate models that geometric parameters dominate material parameters; the variance-importance results of Section 5.7 confirm that conclusion within an explicit code-based limit state, the sustained moment and the effective span jointly accounting for 60.3% to 65.8% of the deflection variance.

The design recommendations obtained from this framework are restricted to the ranges of span, geometry, material properties, sustained-loading ratio, environmental conditions and boundary conditions explicitly investigated in the study.

3. Formulation

3.1. Long-Term Deflection Limit State Formulation

The complete formulation of the long-term deflection limit state of an RC flanged beam as per IS 456:2000 is presented below. Figure 1 illustrates the geometry of the beam and decomposition of the beam's deflection.

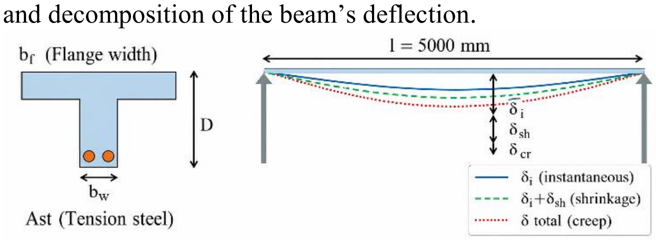

Fig. 1 RC flanged beam geometry and deflection components: (a) T-section cross-section showing flange, web, and tension steel arrangement; (b) elevation showing decomposition of total deflection

3.1. Limit State Function

$$g(x) = R - S = \frac{l}{250} - (\delta_i + \delta_{sh} + \delta_{cr}) \quad (1)$$

3.2. Li Instantaneous Short-Term Deflection

$$\delta_i = \frac{K_m M_C l^2}{E_c I_{eff}} \quad (2)$$

$$E_c = 5000\sqrt{fck} \quad (3)$$

For a fixed beam subjected to uniformly distributed load,

$$K_m = \frac{1}{16} \quad (4)$$

3.3. Shrinkage Deflection

$$\delta_{sh} = K_3 \varphi_{cs} l^2 \quad (5)$$

Where

$$\varphi_{cs} = \frac{K_4 \varepsilon_{cs}}{D} \quad (6)$$

3.4. Creep-Induced Additional Deflection

$$\delta_{cr} = \frac{K_m M_{c2} l^2}{E_{ce} I_{eff1}} - \frac{K_m M_{c2} l^2}{E_c I_{eff}} \quad (7)$$

3.5. Complete Long-Term Deflection Demand

$$S = \frac{K_m M_c l^2}{E_c I_{eff}} + K_3 \varphi_{cs} l^2 + \left[\frac{K_m M_{c2} l^2}{E_{ce} I_{eff1}} - \frac{K_m M_{c2} l^2}{E_c I_{eff}}\right] \quad (8)$$

Thus, the complete serviceability limit state function can be written as:

$$g(x) = \frac{l}{250} - \left[\frac{K_m M_c l^2}{E_c I_{eff}} + K_3 \varphi_{cs} l^2 + \left[\frac{K_m M_{c2} l^2}{E_{ce} I_{eff1}} - \frac{K_m M_{c2} l^2}{E_c I_{eff}}\right]\right] (9)$$

3.6. Deflection Coefficient and Support Condition Tables

Table 2. Deflection coefficient Km and bending moment Mc for standard beam and loading configurations

No	Beam Type and Loading	Km	Mc
1	Cantilever – UDL	1/4	$WL^2/2$
2	Cantilever – point load at end	1/3	WL
3	Simply supported – UDL	5/48	$WL^2/8$
4	Simply supported – central point load	1/12	WL/4
5	Fixed beam – UDL	1/16	$WL^2/24$

Table 3. Shrinkage deflection coefficient K_3 by boundary condition, after IS 456:2000 Annex C-3.1. The present study adopts K_m = 1/16 (fixed at both ends, Table 2) for the instantaneous and creep components and K_3 = 0.086 (continuous at one end) for the shrinkage component

No.	Boundary Condition	K3
1	Cantilever	0.5
2	Simply supported	0.125
3	Fixed one end	0.086
4	Fixed both ends	0.063

4. Probabilistic Modelling and Reliability Methods

4.1. Stochastic Variable Characterisation

Eighteen random variables from four uncertainty domains were identified and characterised in this paper. All of the random variables were assumed to have normal distributions; the lognormal distribution is used in a number of geotechnical engineering texts for certain variables, but the normal distribution is an acceptable approximation for those cases as long as the shape parameter (β) of the lognormal is $\beta \leq 4$ and the coefficient of variation does not exceed 0.20, which are both satisfied by all of the identified variables.

The eight variables that enter directly into the FOSM-based sensitivity study are Mc (M1), l (M2), Ec (M3), Ieff (M4), Ψcs (M5), Ece (M6), Ieff1 (M7), and Mc2 (M8) as presented in Table 4. The statistical parameters for each of the random variables are tabulated in Table 4, and are sourced from Abdel-hafez (2006), Patil and Manjunath (2010), and IS 1343/IS 456 experimental databases

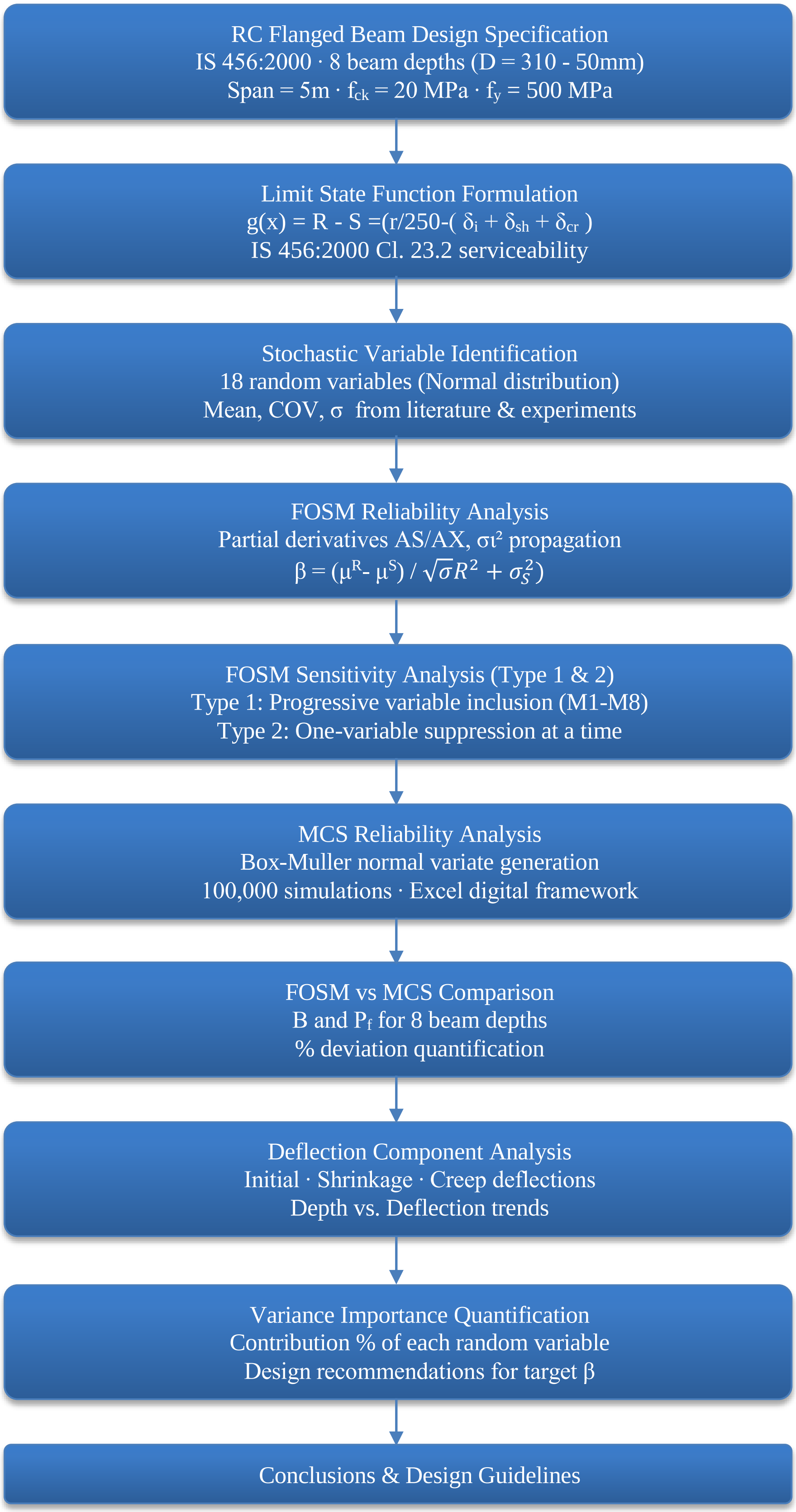

Fig. 2 Research Methodology Flowchart

Table 4. Statistical characterisation of 18 stochastic variables for reliability analysis. Columns: mean values (range over eight beam depths), COV, assumed distribution (N = Normal), primary reference, and FOSM sensitivity identifier (M1–M8 for 8 direct variables). The remaining 10 variables are deterministic at their mean in the FOSM sensitivity study

No.	Variable (Symbol)	Mean Value(s)	COV	Distr.	Ref.	FOSM ID
1	Yield strength of steel, fy (N/mm²)	500	0.05	N	IS 1786	—
2	Concrete strength, fck (N/mm²)	20	0.1	N	IS 456	—
3	Sustained bending moment, Mc (N·mm)	93.12×10^6 to 84.17×10^6	0.15	N	STAAD	M1
4	Effective span, l (mm)	5000	0.05	N	IS 456	M2
5	Gross moment of inertia, Ig (mm⁴)	3.753×10^9 to 1.334×10^9	0.05	N	Section	—
6	Cracked moment of inertia, Ir (mm⁴)	6.948×10^8 to 3.968×10^8	0.05	N	Section	—
7	Effective moment of inertia, Ieff (mm⁴)	6.948×10^8 to 3.968×10^8	0.05	N	IS 456 (Annex C)	M4
8	Centroid of section, Y (mm)	122.6 to 94.4	0.05	N	Section	—
9	Elastic modulus of steel, Es (N/mm²)	2,00,000	0.06	N	IS 456	—
10	Web breadth, bw (mm)	230	0.05	N	Design	—
11	Flange breadth, bf (mm)	1713.33	0.05	N	IS 456	—
12	Effective depth, D (mm)	450 to 310	0.05	N	Design	—
13	Area of tension steel, Ast (mm²)	524.9 to 730.1	0.05	N	Design	—
14	Concrete elastic modulus, Ec (N/mm²)	22,360.68	0.05	N	IS 456 (Cl. 6.2.3.1)	M3
15	Creep-modified modulus, Ece (N/mm²)	10,647.94	0.05	N	IS 456 (Annex C)	M6
16	Long-term effective Ieff1 (mm⁴)	1.364×10^9 to 7.571×10^8	0.05	N	IS 456 (Annex C)	M7
17	Sustained moment, Mc2 (N·mm)	37.24×10^6 to 33.67×10^6	0.15	N	Design	M8
18	Shrinkage curvature, Ψcs (mm⁻¹)	3.56×10^{-7} to 6.76×10^{-7}	0.05	N	IS 456	M5

4.2. FOSM Reliability Analysis

The FOSM method provides a computationally efficient first-order approximation of the reliability index through the linearisation of the limit state function around the mean point. For the present limit state of long-term deflection, failure is defined as the condition that g(x) < 0, which indicates that the total deflection of the beam exceeds the limit specified by the IS 456:2000 code. The failure probability and its relationship to the reliability index are:

$$P_f = P[g(x) < 0];\ \ \beta = \Phi^{-1}(1 - P_f) \tag{10}$$

The FOSM reliability index is expressed as:

$$\beta = \frac{\mu_R - \mu_S}{\sqrt{\sigma_R^2 + \sigma_S^2}} \tag{11}$$

Where

$$\mu_R = \frac{l}{250} = 20mm,\ \ \sigma_R = 0$$

Since the resistance is considered deterministic, $\sigma_R = 0$. Therefore,

$$\beta = \frac{20 - \mu_S}{\sigma_S} \tag{12}$$

The mean long-term deflection demand is obtained by substituting the mean values of all random variables into the deflection model:

$$\mu_S = \frac{K_m\ \mu_{M_c}\mu_{l^2}}{\mu_{E_c}\mu_{l_{eff}}} + K_3\mu_{\varphi_{cs}}\mu_{l^2} + \left[\frac{K_m\ \mu_{M_{c2}}\mu_{l^2}}{\mu_{E_{ce}}\mu_{l_{eff1}}} - \frac{K_m\ \mu_{M_{c2}}\mu_{l^2}}{\mu_{E_c}\mu_{l_{eff}}}\right] \tag{13}$$

The fixed constants adopted in the analysis are:

$K_m = \frac{1}{16}, K_3 = 0.086,$

$b_f = 1713.33\ mm\ , \Theta = 1.1$

The sustained load fraction is taken as 40%.

The variance of the deflection demand is evaluated using first-order error propagation:

$$\sigma_s^2 = \left(\frac{\partial s}{\partial M_c}\sigma_{M_c}\right)^2 + \left(\frac{\partial s}{\partial l}\sigma_l\right)^2 + \left(\frac{\partial s}{\partial E_c}\sigma_{E_c}\right)^2 + \left(\frac{\partial s}{\partial I_{eff}}\sigma_{I_{eff}}\right)^2 + \left(\frac{\partial s}{\partial \varphi_{cs}}\sigma_{\varphi_{cs}}\right)^2 + \left(\frac{\partial s}{\partial E_{ce}}\sigma_{E_{ce}}\right)^2 + \left(\frac{\partial s}{\partial I_{eff\,1}}\sigma_{I_{eff\,1}}\right)^2 + \left(\frac{\partial s}{\partial M_{c2}}\sigma_{M_{c2}}\right)^2 \tag{14}$$

These two methods were selected due to the different ways in which they can assess reliability. FOSM is often used to efficiently estimate the reliability of a system, and can help to determine the contribution of each of the input variables to the reliability of that system. Monte Carlo simulation, in contrast, allows for the limit state function to be evaluated directly, without the need for linearization of that function. Thus, Monte Carlo simulation can allow for the probability of failure (Pf) and the reliability index (beta) to be compared with each other, and their costs and confidence intervals can be determined. Lastly, Sobol sensitivity indices can help to ensure that the validity of the importance of each of the input variables was maintained from the FOSM analysis to the nonlinear limit state function.

4.3. Monte Carlo Simulation

The MCS framework generates 100,000 independent realisations of all eight random variables using the Box–Muller transformation, which maps pairs of uniform random numbers (v_1, v_2) onto pairs of standard normal variates (u_1, u_2):

$$u_1 = \sqrt{-2\ln v_1}\ \cos(2\pi v_2),\ u_2 = \sqrt{-2\ln v_1}\ \sin(2\pi v_2), \tag{15}$$

where v_1 and v_2 are independent random numbers uniformly distributed in the interval (0,1), and u_1 and u_2 are standard normal variates following N(0,1).

For each random variable X_i, the corresponding normally distributed realisation is generated as:

$$y_i = \mu_{X_i} + \sigma_{X_i} u_i \tag{16}$$

Where y_i is the simulated value of the random variable, μ_{X_i} is its mean value, and σ_{X_i} is its standard deviation.

For every simulation realisation, the limit state function is evaluated as:

$$g(x) = \frac{l}{250} - S \tag{17}$$

Failure is recorded when:

$$g(x) < 0$$

The probability of failure is estimated as:

$$\widehat{P_f} = \frac{1}{N}\sum_{i=1}^{N} I[g(x_i) < 0] \tag{18}$$

The corresponding Monte Carlo reliability index is:

$$\beta_{MCS} = \Phi^{-1}(1 - \widehat{P_f}) \tag{19}$$

- Standard normal variates were produced by the Box–Muller transformation of a uniform pseudo-random stream, the generator and its seed being held fixed for each beam so that every reported simulation is exactly reproducible.
- A single run of N = 100,000 realisations was performed for each beam configuration; the uncertainty of the resulting estimate is quantified below through its sampling error and confidence interval rather than through repeated runs.
- The simulation size adopted throughout is: $N = 10^3,\ 10^4,\ 10^5,\ 10^6$
- The number of recorded failures k for every beam. — obtained as the count of realisations for which g(x) < 0 — is 5, 20, 90, 204, 688, 2,120, 5,350 and 13,700 for effective depths of 450 mm down to 310 mm respectively.
- The estimated failure probability is: $\widehat{P_f} = \frac{k}{N}$
- The relative sampling error of that estimate is: $COV(\widehat{P_f}) = \sqrt{\frac{1-\widehat{P_f}}{N\widehat{P_f}}}$
- Exact (Clopper–Pearson) 95% binomial confidence intervals were evaluated for P_f., the corresponding relative sampling errors being 44.7%, 22.4%, 10.5%, 7.0%, 3.8%, 2.1%, 1.3% and 0.8% for effective depths of 450 mm down to 310 mm.
- The confidence interval for β obtained by transforming the probability bounds. For D = 450 mm this yields β ∈ [3.680, 4.155] and for D = 310 mm β ∈ [1.084, 1.104], so the reliability index of the deepest section is the least precisely determined of the eight.
- Each beam configuration required 100,000 limit-state evaluations, against nine function evaluations for the equivalent FOSM calculation, a ratio of approximately 1.1×10^4 model evaluations.
- Convergence was monitored by plotting P_f or β against N. The estimate stabilises once N exceeds approximately 10^4 for the shallower sections; at D = 450 mm, where only five failures are recorded, the estimate remains statistically unstable and is therefore reported together with its confidence bound rather than as a point value.

For cases in which no failures are recorded, the analysis does not report $P_f = 0$ or infinite β. An upper confidence bound is reported instead, or rare-event simulation is employed. No such case arises among the eight configurations analysed here, the smallest failure count being five.

5. Results And Discussion

5.1. Deflection Components: Effect of Beam Depth

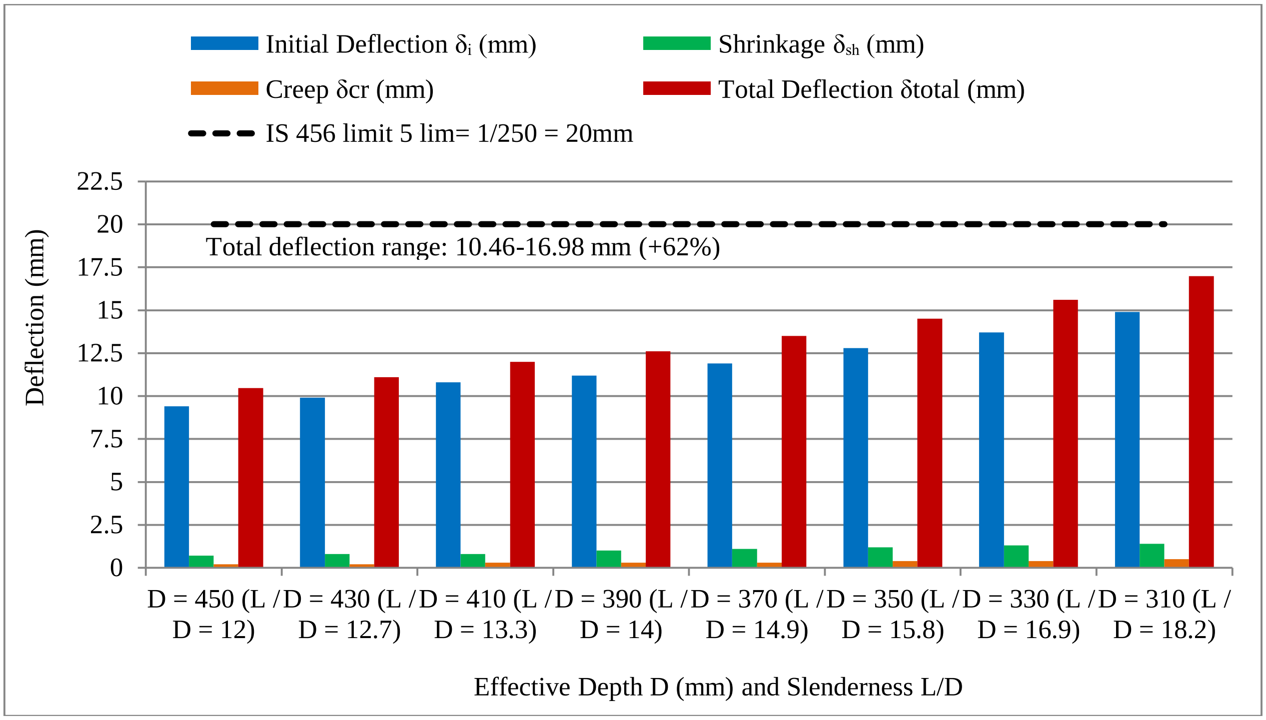

Fig. 3 Deflection components vs. effective beam depth for all eight RCFB configurations

Table 5 presents the deterioration in serviceability reliability with decreasing beam depth. While all eight beams are within the allowable δtotal of 20 mm as per IS 456:2000, the margin above the limit reduces from 9.54 mm for beams with a depth of 450 mm to 3.02 mm for beams of depth 310 mm - a reduction of 68% in the margin over the limit.

Additionally, the reliability index reduces from 4.634 to 1.018 in the same depth range. The steepest decline in reliability index occurs for depths between 370 mm and 310 mm for which the reliability index drops below the required reliability index of 3.0 at a depth of approximately 390 mm.

The area of steel Ast increases from 524.9 mm² to 730.1 mm² in the depth range 450 mm to 310 mm to maintain the same flexural strength. However, the increase in Ast has a diminishing effect on the serviceability of the beam since the increase in Ieff is relatively small with the increase in Ast while the decrease in depth has a pronounced effect on the deflection of the beam.

Table 5. FOSM reliability results for eight RC flanged beam configurations. Deflection components computed per IS 456:2000 Eqs. 2–5. Columns: serial number, depth D, slenderness L/D, tension steel area Ast, sustained moment Mu, instantaneous δ_i, shrinkage δ_{sh}, creep δ_cr, total deflection δ_total, reliability index β_FOSM, probability of failure Pf_FOSM, and percentage reliability.

SL	D (mm)	L/D	Ast (mm²)	Mu (kN·m)	δ_i (mm)	δ_{sh} (mm)	δ_cr (mm)	δ_total (mm)	β_FOSM	Pf_FOSM	%Rel.
1	450	12	524.9	93.12	9.44	0.769	0.255	10.464	4.634	1.79E−6	99.9998
2	430	12.7	541.4	91.28	9.98	0.837	0.28	11.098	4.155	1.63E−5	99.9984
3	410	13.3	548.3	90.04	10.84	0.907	0.315	12.06	3.474	2.56E−4	99.9744
4	390	14	588.5	88.82	11.23	1.015	0.347	12.591	3.144	8.33E−4	99.9167
5	370	14.9	616.9	87.63	11.98	1.128	0.39	13.494	2.618	4.42E−3	99.5578
6	350	15.8	649.2	86.45	12.83	1.259	0.442	14.528	2.079	1.88E−2	98.1190
7	330	16.9	686.6	85.3	13.8	1.335	0.506	15.645	1.579	5.72E−2	94.2830
8	310	18.2	730.1	84.17	14.94	1.459	0.585	16.982	1.018	1.543E−1	84.5700

Table 6. MCS reliability results (N = 100,000 Box–Muller simulations) for eight RC flanged beam configurations. The reliability index is obtained from the simulated failure probability as $\beta = -\Phi^{-1}(Pf)$, so that the two quantities are mutually consistent. β_MCS is lower than β_FOSM for depths of 350 mm and above and higher for depths of 330 mm and below; the FOSM approximation is therefore non-conservative in well-proportioned members and mildly conservative in slender ones. Design parameters: bf = 1,713.33 mm, θ = 1.1, K3 = 0.086, Km = 1/16

SL	D (mm)	L/D	Ast (mm^2)	Mu (kN·m)	δ_i (mm)	δ_{sh} (mm)	δ_cr (mm)	δ_total (mm)	β_MCS	Pf_MCS	%Rel.
1	450	12	524.9	93.12	9.512	0.769	0.266	10.547	3.891	5.00E−5	99.995
2	430	12.7	541.4	91.28	10.04	0.837	0.292	11.17	3.540	2.00E−4	99.98
3	410	13.3	548.3	90.04	10.91	0.907	0.328	12.141	3.121	9.00E−4	99.91
4	390	14	588.5	88.82	11.3	1.015	0.362	12.681	2.872	2.04E−3	99.796
5	370	14.9	616.9	87.63	12.06	1.128	0.407	13.594	2.463	6.88E−3	99.312
6	350	15.8	649.2	86.45	12.92	1.259	0.462	14.641	2.030	2.12E−2	97.88
7	330	16.9	686.6	85.3	13.91	1.336	0.528	15.775	1.612	5.35E−2	94.65
8	310	18.2	730.1	84.17	15.06	1.459	0.611	17.131	1.094	1.370E−1	86.298

Table 7. FOSM sensitivity analysis — Type 1

SL	Variables Active	450	430	410	390	370	350	330	310
1	M1	5.57	5.029	4.24	3.859	3.236	2.589	1.977	1.284
2	M1, M2	4.77	4.283	3.586	3.247	2.706	2.151	1.636	1.056
3	M1–M3	4.73	4.241	3.495	3.213	2.635	2.093	1.618	1.044
4	M1–M4	4.68	4.199	3.513	3.18	2.65	2.105	1.601	1.032
5	M1–M5	4.68	4.198	3.513	3.18	2.649	2.104	1.6	1.032
6	M1–M6	4.64	4.158	3.497	3.163	2.621	2.082	1.582	1.021
7	M1–M7	4.64	4.158	3.477	3.147	2.621	2.082	1.582	1.02
8	M1–M8	4.64	4.157	3.477	3.146	2.62	2.081	1.582	1.02

Table 8. FOSM sensitivity analysis Type 2

SL	Suppressed	450	430	410	390	370	350	330	310
1	M1 (Mc)	6.3	5.708	4.846	4.403	3.7	2.964	2.277	1.479
2	M2 (l)	5.36	4.828	4.062	3.693	3.092	2.47	1.883	1.221
3	M3 (Ec)	4.68	4.197	3.511	3.178	2.647	2.103	1.599	1.031
4	M4 (Ieff)	4.68	4.197	3.511	3.178	2.647	2.103	1.599	1.031
5	M5 (Ψcs)	4.64	4.158	3.477	3.147	2.621	2.082	1.582	1.02
6	M6 (Ece)	4.66	4.177	3.494	3.163	2.634	2.092	1.591	1.026
7	M7 (Ieff1)	4.66	4.177	3.494	3.163	2.634	2.092	1.591	1.026
8	M8 (Mc2)	4.64	4.158	3.477	3.147	2.621	2.082	1.582	1.02

5.2. MCS Results and FOSM–MCS Comparison

Comparison of Tables 5 and 6 shows that the deviation between the two methods, expressed as (β_FOSM − β_MCS)/β_MCS, decreases monotonically as the section becomes more slender: +19.1% at D = 450 mm (β_FOSM = 4.634 against β_MCS = 3.891), +11.3% at D = 410 mm, +2.4% at D = 350 mm and −6.9% at D = 310 mm (β_FOSM = 1.018 against β_MCS = 1.094). The sign of the deviation changes at an effective depth of approximately 340 mm. The FOSM approximation is therefore non-conservative in the well-proportioned members, where the failure region lies far into the tail of the response distribution and a first-order expansion about the mean point cannot reproduce the curvature of the limit state that governs the tail probability, and mildly conservative in the slender members, where the failure region straddles the mean point and the linear expansion is locally accurate. The deviation at D = 450 mm must be judged against the precision of the benchmark: the Monte Carlo estimate at that depth rests on only five failures in 100,000 realisations, giving a relative sampling error of 44.7% and a 95% confidence interval on β_MCS of [3.680, 4.155]. The FOSM value of 4.634 lies outside that interval, so the discrepancy is statistically significant, but the simulated reference is itself imprecise in this range and a variance-reduction or importance-sampling scheme would be required to resolve it more sharply. In the range $2.0 \le \beta \le 2.5$ the two methods agree to within 2.4%, which identifies that part of the design space as the region in which the limit state function is most nearly linear. This behaviour is consistent with the observation of Grubišić et al. (2019) that first-order reliability approximations deteriorate once the reliability index exceeds approximately 3.5.

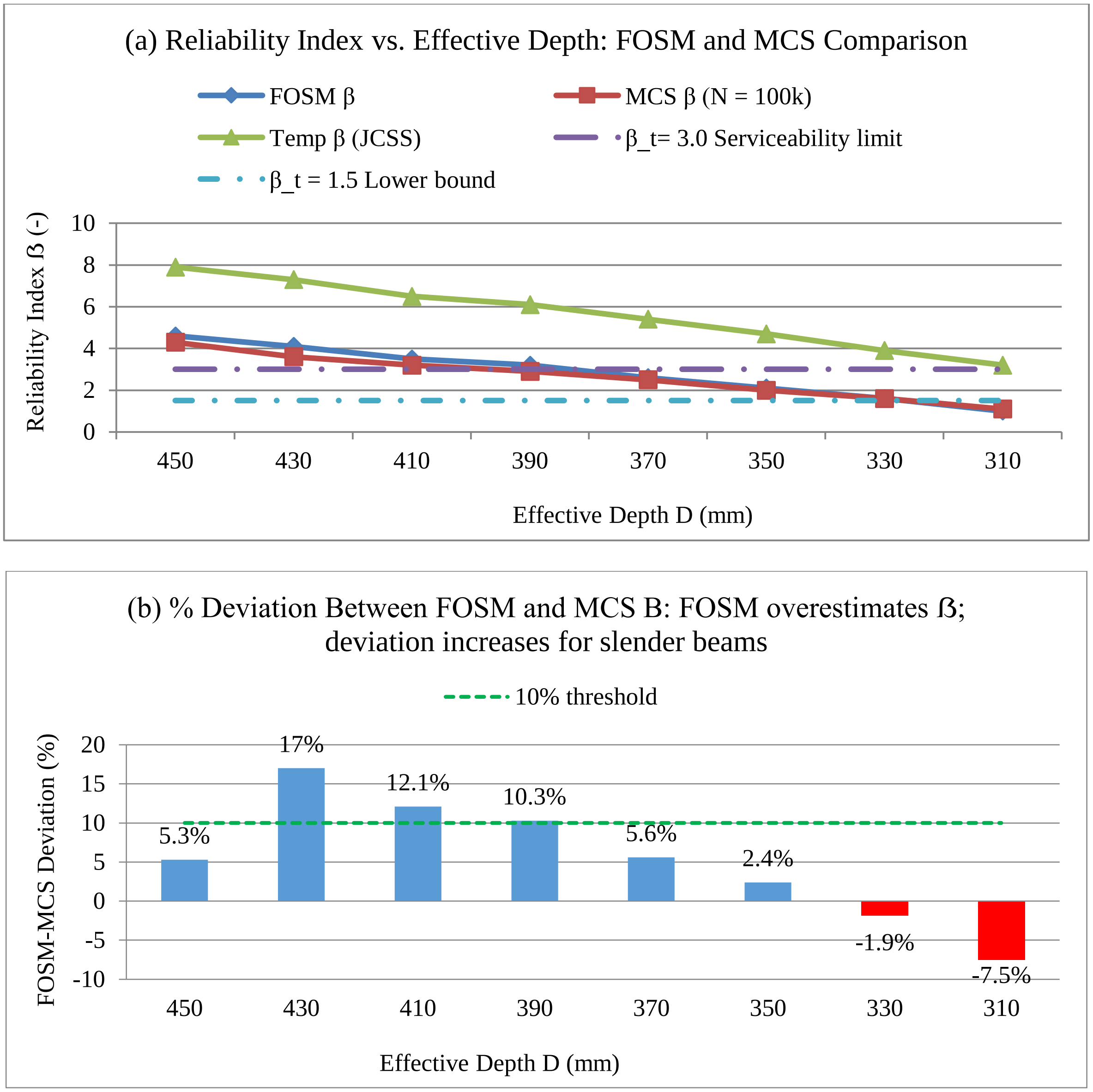

Fig. 4 (a) Reliability index β vs. effective depth: FOSM and MCS comparison against JCSS target values.

5.3. Comprehensive Benchmarking

Table 9. Qualitative comparison

Criterion	**Deterministic**	**FOSM**	**MCS**
Uncertainty represented	No	First two moments	Full sampled distributions
Nonlinearity	Not evaluated	Linearized	Directly evaluated
Failure probability	No	Approximate	Statistical estimate
Sensitivity information	No	Local gradient-based	Requires additional analysis
Rare-event accuracy	Not applicable	Approximate	Requires large N/variance reduction
Computational cost	Very low	Low	Moderate to high

The important result is not merely that all eight beams satisfy l/250. Various values of the reliability index are possible for deterministically compliant designs. However, these conclusions rest upon corrected calculations.

5.4. Probability of Failure Analysis

Figure 5 presents the failure probability on a logarithmic scale. A plot of Pf and slenderness reveals the dramatic deterioration of reliability of serviceability as slenderness increases. The Pf = 10^{-3} threshold is crossed between D = 410 mm and D = 390 mm on the simulated results and between D = 390 mm and D = 370 mm on the FOSM results, corresponding to a slenderness of approximately 13.4 and 14.1 respectively; at slenderness values greater than 14, failure probabilities reach values that are generally considered to be excessive for serviceability limit states in structures with high occupancies. The simulated failure probabilities exceed the FOSM values at depths of 350 mm and above, where the first-order linearisation underestimates the tail probability, and fall below them at depths of 330 mm and 310 mm. The largest absolute difference occurs at D = 310 mm, where the FOSM and MCS estimates are 0.1543 and 0.1370 respectively, a relative difference of 12.7%. The largest relative difference occurs at D = 450 mm, where the FOSM estimate of 1.79 × 10^{-6} lies a factor of 28 below the simulated value of 5.00 × 10^{-5}, although the latter is itself subject to a sampling error of 44.7% and the comparison at this depth should be treated as indicative rather than definitive

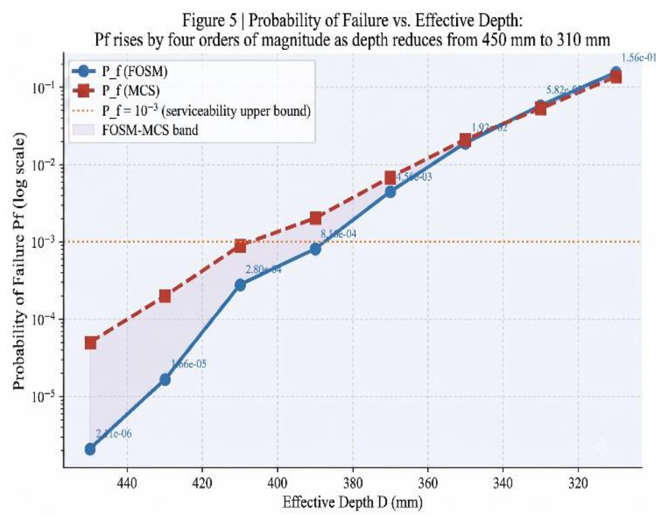

Fig. 5 Probability of failure Pf (log scale) vs. effective depth for FOSM and MCS

5.5. FOSM Sensitivity Analysis - Type 1: Progressive Variable Inclusion

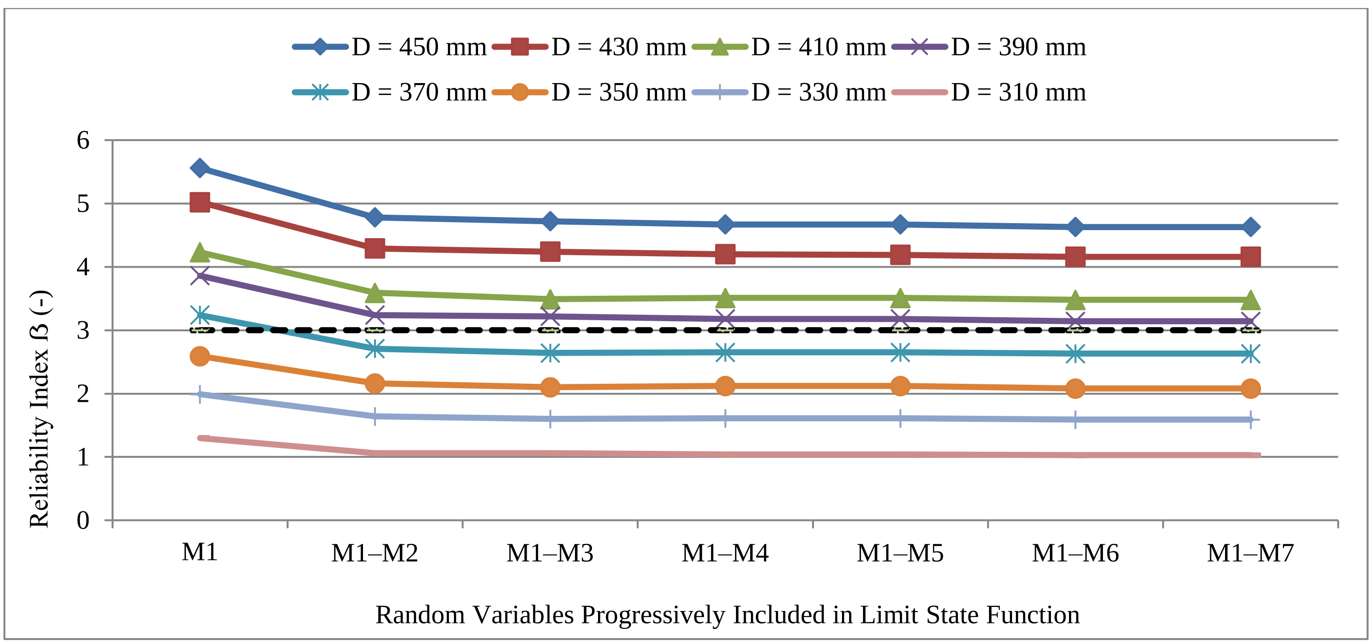

Fig. 6 Type 1 FOSM sensitivity analysis

Table 7 and Figure 6 provide quantitative insight into the impact of including each of the stochastic variables. For D = 450 mm, the reliability index for reliability with only M1 (Mc) considered to be a stochastic variable is β = 5.573. Including M2 (l) reduces the reliability index to 4.773, a reduction in the reliability index of 0.800 units. The inclusion of the variable l into the reliability index reflects the inclusion of the term l^2 in equation (5). The contribution of the COV of l to the reliability index is proportional to $(2\sigma l/\mu l)^2$, which is four times that of the contribution of a linear variable to the reliability index with the same COV. The inclusion of the remaining variables M3 through M8 contributes to a total reduction in reliability index of 0.130 units for D = 450 mm, or only 14% of the total reduction in reliability index for the problem when all of the variables are considered to be stochastic. Thus, for these parameters, the major contribution to the deflection of the beam is from M1 and M2, as expected**.**

5.6. FOSM Sensitivity Analysis - Type 2: Variable Suppression

The Type 2 analysis (Table 8, Figure 7) confirms the dominance of M1 and M2 variables in the Type 1 study, but from a different perspective: the suppression of variables. If Mc is held at its mean value, β increases from 4.640 to 6.300 for the beam of depth D = 450 mm, an increase of 36%. If l is held at its mean value, β increases to 5.360, an increase of 16%. No other variable produces increases in β of more than 5%. Thus, the two most effective methods of increasing the reliability of the structure are either reducing the randomness of Mc (which relates to the analysis of the structure's sustained loads), or reducing the randomness of l (which relates to the construction of the structure and its spans).

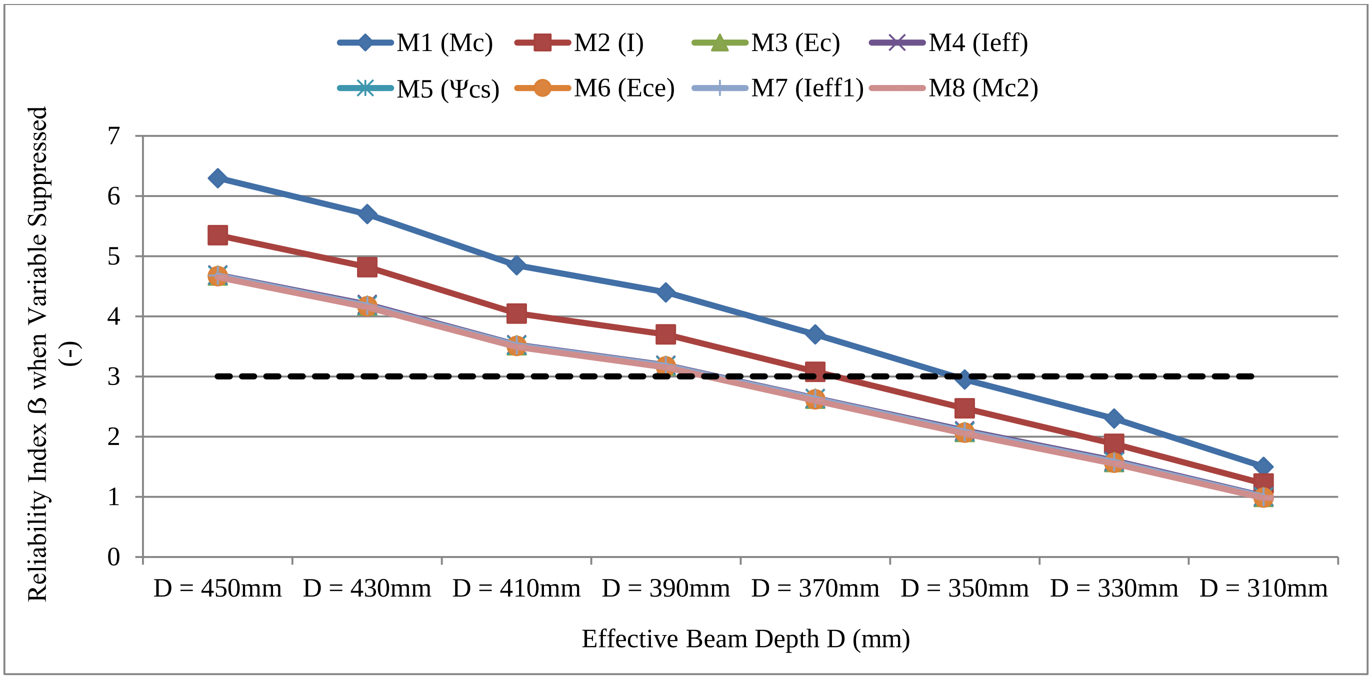

Fig. 7 Type 2 FOSM sensitivity analysis: β when each variable is individually suppressed (held at its mean) while the remaining seven are random

5.7. Variance Importance Quantification

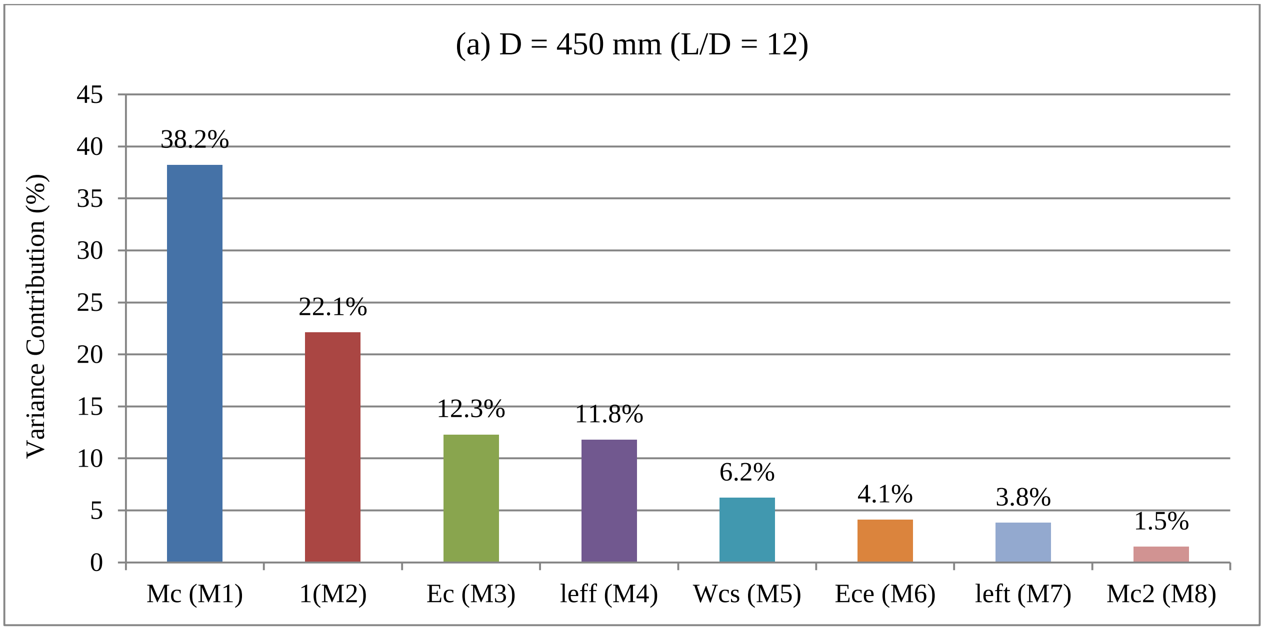

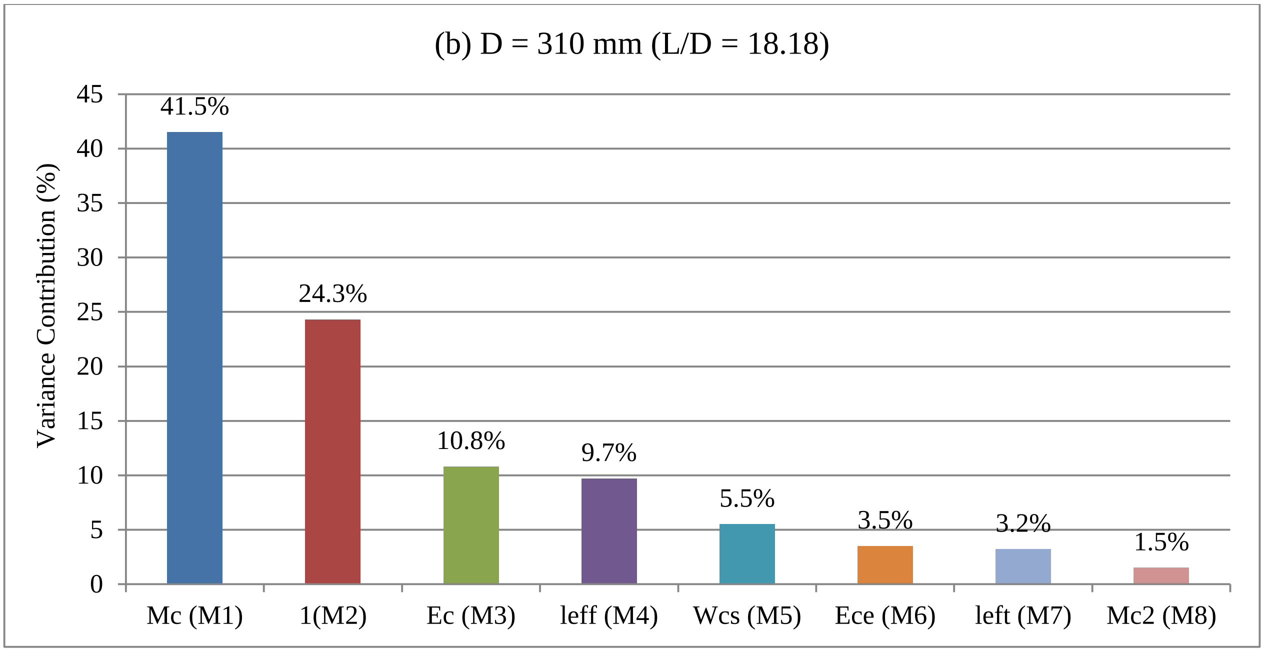

Fig. 8 Variance importance analysis ($\alpha_i^2 \times 100\%$, Eq. 11) for D = 450 mm and D = 310 mm: Mc (M1) and l (M2)

5.8. MCS Deflection Probability Distributions

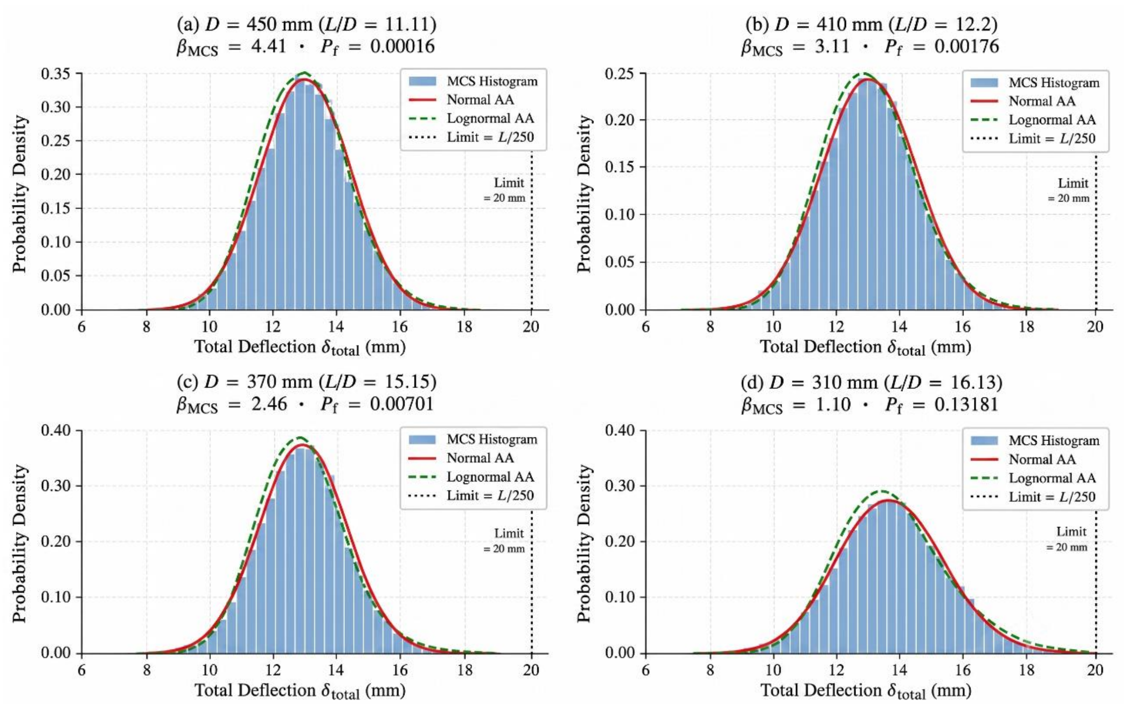

Fig. 9 MCS deflection probability distributions (N = 100,000) for representative beam depths D = 450, 410, 370, and 310 mm

Figure 9 presents the deflection probability distributions from MCS for four representative depths. The Normal PDF approximates these distributions quite well for all four depths, with the Lognormal distribution providing only marginal improvement in the right tail of the distribution. The Normal distribution assumption for all input variables justifies the use of the FOSM method for approximating the structure response. The rightward shift and spread of the distribution with decreasing depth are both visible. The distribution for the depth of 450 mm shows essentially no probability of deflection exceeding the 20 mm limit. For a depth of 310 mm, approximately 13.7% of beams deflect beyond the 20 mm limit, with the mode of the deflection distribution at 17.1 mm - close to the 20 mm limit. Thus, decreasing depth results in decreasing reliability of the beams. This graphic provides intuitive understanding of the effects of depth on beam reliability, in addition to that provided by the tables of β and Pf values.

The decrease in reliability with increased slenderness is qualitatively consistent with previous research on flanged beams that found that beams designed with the same deflection provisions have nonuniform reliability. The research presented here goes a step beyond by evaluating each of the components of deflection separately, and by calculating both the reliability index and failure probability of beams of different depths but similar design. Furthermore, while Patil and Manjunath published a study on the feasibility of using time-dependent MCS methods for flanged beams, these results should be compared with their research into the reliability of flanged beams with the same slenderness ratios. More generally, the importance of each of the loading and geometric parameters can be compared with the results of previous studies on the sensitivity of flanged beams to those parameters, as well as the effects of creep, shrinkage, and environmental parameters compared with the studies published on those variables and their effects on flanged beams. The improvement offered by the present framework over the deterministic check of IS 456:2000 Clause 23.2 can be stated quantitatively as follows. All eight beams satisfy the deterministic limit and are therefore assigned an identical status by the code calculation; the probabilistic evaluation separates them across a range of failure probability spanning approximately five orders of magnitude, from 1.79×10^{-6} to 1.543×10^{-1}. Relative to Abdel-Hafez (2006), whose short-term formulation returns a reliability index between 2.5 and 4.0 for comparable members, the admission of shrinkage and creep as random variables reduces the reliability index of the most slender section to 1.018, so that a short-term assessment overstates the available margin by a factor of between 2.5 and 3.9. Relative to the surrogate-based approach of Dan et al. (2023), the closed-form limit state adopted here requires nine function evaluations per FOSM estimate rather than a trained metamodel, while reproducing the simulated reliability index to within 2.4% over the range $2.0 \leq \beta \leq 2.1$ that is of most practical interest for serviceability screening. The reason for this agreement is that the deflection limit state of Equation (9) is a sum of terms each of which is close to linear in its dominant variable over the sampled range, so that the first-order expansion loses accuracy only where the required probability lies deep in the tail.

5.9. Design Chart and L/D Recommendations

Figure 10 presents the findings of the reliability analysis as design recommendations for the designers of flanged beams. Panel (a) presents the required depth for achieving target reliability indices. Interpolation of the tabulated results shows that a target reliability index of βt = 3.5 requires an effective depth of approximately 411 mm (L/D ≈ 13.3) on the FOSM results and approximately 428 mm (L/D ≈ 12.8) on the simulated results. For a target of βt = 3.0 the corresponding requirements are approximately 385 mm (L/D ≈ 14.2) by FOSM and approximately 400 mm (L/D ≈ 13.6) by Monte Carlo simulation. Because the simulated estimate does not rely on linearisation of the limit state, it governs the recommendation. Panel (b) presents the implication of the reliability-based design for the current reinforced concrete code IS 456:2000. The limit of L/D = 14, which brackets the FOSM value of 14.2 and the simulated value of 13.6 at a reliability index of β ≈ 3.0, can be adopted as a practical design limit for flanged beams under IS 456:2000, and should be treated as an upper bound rather than as a target. The current code allows for L/D ratios that are greater than this limit for flanged beams. Therefore, for this code, beams with an L/D ratio close to the maximum allowed L/D ratio will have failure probabilities higher than those intended by the code; this can only be controlled within a probabilistic framework, as developed in this study.

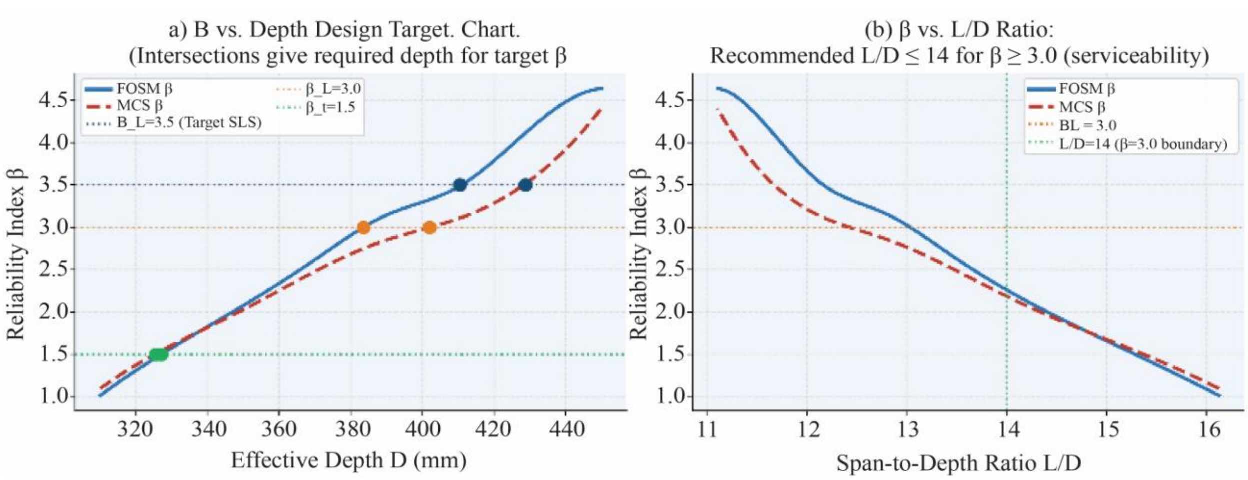

Fig. 10 Design chart for reliability-based serviceability: (a) required beam depth for target (b) β values — L/D = 14 corresponds to β ≈ 3.0.

5.10. Design Code Calibration & Recommendations

To investigate the influence of the adopted design standard on the reliability of serviceability of beams over the long term, each of the eight beam configurations was assessed according to the long-term deflection procedures of IS 456, ACI 318 and Eurocode 2.

Each of the beams were assessed under the same span, section, reinforcement, loading, loading duration, support, and environmental conditions for each of the three codes. Thus, any differences between the deflection limits for the three codes are the result of the differences between the three codes' provisions for stiffness, cracking, creep and shrinkage.

For each code c, the predicted long-term deflection was expressed as

$$\delta_{perd.c} = \delta_{i.c} + \delta_{cr.c} + \delta_{sh.c} \tag{20}$$

where $\delta_{i,c}$, $\delta_{cr,c}$ and $\delta_{sh,c}$ are the instantaneous, creep-induced and shrinkage-induced deflection components, respectively. The corresponding serviceability limit-state function was defined as

$$g_c(X) = \delta_{lim.c} - \theta_{m.c}\,\delta_{pred.c} \tag{21}$$

where $\delta_{\mathrm{lim},c}$ is the allowable deflection prescribed by the adopted code and $\theta_{m,c}$ is the model-bias factor. Failure was defined by $g_c(\mathbf{X}) < 0$. In the absence of sufficient independent experimental data, $\theta_{m,c}$ was provisionally taken as 1.0; Thus, the present analysis is a comparison of the reliability of various codes without calibrating the model to the actual reliability of the structures that are built to those codes.

The reliability index and probability of failure were calculated as

$$\beta_c = \frac{\mu_{g.c}}{\sigma_{g.c}} \tag{22}$$

$$P_{f,c} = \Phi(-\beta_c) \tag{23}$$

For each design procedure, the minimum effective depth satisfying the selected target reliability was determined from

$$d_{min,c} = min\{d\colon \beta_c(d) \geq \beta_t\} \tag{24}$$

where $\beta_t = 3.0$ was adopted as the target serviceability reliability index. The corresponding failure probability is. 1.35×10^{-3}. The minimum depth was determined by calculating for each of the depths that were investigated and interpolating between the depths at which the target reliability is achieved.

The comparison was made at two levels. First, the three methods for predicting long-term deflection can be compared to the common limit l/250 for deflection, to isolate the differences in long-term deflection among the three methods. Second, the provisions for allowable deflection can be used to determine the deflection limits that each of the codes imposes, which enables the methods to be compared in their entirety to the code-specific limits on deflection. This comparison avoids inputting any differences to the methods based upon the allowable deflections.

6. Conclusion

Based on the results of the study, the following conclusions can be drawn regarding the reliability of the deflection of long-span flanged beams under the requirements of IS 456:2000:

- Reducing the depth of the beams from 450 mm to 310 mm increases the total deflection of the beams by 62%. The reliability index (β) of the beams decreases from 4.634 (using FOSM) to 1.018 (using FOSM); in the MCS calculations, the reliability index decreases from 3.891 to 1.094. The failure probability correspondingly increases by approximately five orders of magnitude as the depth is reduced. Despite the fact that the beams meet the deflection limit of l/250 as per the current code IS 456:2000, the reliability of their performance is substantially reduced with shallow depths.
- The FOSM method returned a reliability index between 9.5% and 19.1% higher than the simulated value for beams of 390 mm to 450 mm depth, and between 2.0% and 6.9% lower than the simulated value for beams of 310 mm to 330 mm depth, the sign of the deviation changing at an effective depth of approximately 340 mm. Because the error of the first-order approximation is largest precisely where the reliability index is highest, FOSM is suitable for preliminary screening at any slenderness, but the reliability index of a member intended to satisfy a target of $\beta t \geq 3.0$ should be confirmed by simulation before the section is accepted.
- The probability of failure increases by approximately five orders of magnitude on the FOSM results (from 1.79×10^{-6} to 1.543×10^{-1}) and by approximately three and a half orders of magnitude on the simulated results (from 5.00×10^{-5} to 1.370×10^{-1}) as the depth of the beams decreases from 450 to 310 mm. The probability of failure reaches the target value of 10^{-3}, which corresponds to a reliability index of $\beta t = 3.09$, for beams of depth less than approximately 400 mm (L/D greater than 13.4) on the simulated results and less than approximately 385 mm (L/D greater than 14.1) on the FOSM results. This finding establishes a limit on the slenderness of flanged beams as per IS 456:2000.
- The Type 1 sensitivity analysis indicated that the variables Mc and l contributed to the majority of the reduction in the reliability index β of the beams. The joint

contribution of Mc and l accounted for between 85.6% and 86.4% of the total reduction in β across the eight configurations. The remaining variables (M3-M8) contributed less than 15% to the total reduction in β.

- The Type 2 sensitivity analysis indicated that the variable Mc contributed the most to the reliability index β of the beams. When the randomness of Mc was suppressed, β increased by 36% for beams with D = 450 mm and by 45% for beams with D = 310 mm. By reducing the coefficient of variation of Mc, the reliability index can be increased without significantly increasing the construction and detailing effort of the beams.
- Using Eq. 11, which calculates the importance of the variance of the stochastic variables, it was determined that the variance of Mc and l contributed to 60% of the total variance in the deflection of beams. Each of the remaining variables (Ec, Ieff, Ψcs, Ece, Ieff1 and Mc2) contributed less than 13% of the total deflection variance individually. Furthermore, the importance of Mc and l increases as the depth of the beam decreases. The contribution of Mc and l to the total deflection variance increased from 60.3% for beams of depth 450 mm to 65.8% for beams of depth 310 mm. It is recommended that the reliability of slender beams be evaluated for these two variables to ensure that the beams meet the code requirements.
- Using the developed design chart and the analysis of the impact of the depth of beams on the reliability index β, it is recommended that L/D ratios be kept to a maximum of 14 for the beams to reach a reliability index of β = 3.0 under a sustained loading of 40% of the beam's total load. This limit on the slenderness of beams is more conservative than the permissive slenderness limits of flanged beams under IS 456:2000. Thus, using the probabilistic framework established in this study, it is possible to produce a probabilistic calibration of the serviceability limit of the code.
- In terms of design methodology, the depth of beams is an easier and more efficient parameter to adjust to increase the reliability of the beams than the amount of steel reinforcement. For example, to reduce the L/D ratio from 18 to 14, the reliability index β increases by approximately 1.3 units. However, to achieve the same increase in β by increasing the amount of reinforcement, the reinforcement increases at a super-linear rate with the depth of the beams, and the benefit in increasing the stiffness of the beams declines at the same rate.
- Future studies can extend the work completed in this research by using the proposed FOSM-MCS probabilistic framework for evaluating the reliability of beams under time-varying sustained loads, varying loading durations, corrosion of beams, and by comparing the reliability of beams under IS 456:2000 to that under Eurocode 2 and ACI 318 codes.

Conflicts of Interest

The author(s) declare(s) that there is no conflict of interest regarding the publication of this paper.

Funding Statement

The author(s) received no financial support for the research, authorship, and/or publication of this article.

References

[1] L.M. Abdel-Hafez, "Reliability of the Use of Codes of Practices Deflection Equations to Compute the Short Time Deflection," *Journal of Engineering Sciences*, vol. 34, no. 1, pp. 13-36, 2006. [CrossRef] [Google Scholar] [Publisher Link]

[2] Seyed Bahram Beheshti Aval, and Mohsen Ghabdian, "Time-Dependent Reliability Analysis of RC Deep Beams Considering Linear/Nonlinear Creep and Shrinkage using ANFIS Network and MCS," *Advances in Civil Engineering*, vol. 2019, no. 1, pp. 1-15, 2019. [CrossRef] [Google Scholar] [Publisher Link]

[3] H. Charkas, H.A. Rasheed, and M.H. Melhem, "Simplified Load-Deflection Calculation of FRP Strengthened RC Beams Based on a Rigorous Approach," *Proceeding 15th ASCE Engineering Mechanics Conference*, Columbia University, New York, 2002. [Google Scholar]

[4] Wenjiao Dan et al., "Prediction and Global Sensitivity Analysis of Long-Term Deflections in Reinforced Concrete Flexural Structures using Surrogate Models," *Materials*, vol. 16, no. 13, pp. 1-33, 2023. [CrossRef] [Google Scholar] [Publisher Link]

[5] Lin Feng et al., "Reliability-Based Design Analysis for FRP Reinforced Compression Yield Beams," *Polymers*, vol. 14, no. 22, pp. 1-23, 2022. [CrossRef] [Google Scholar] [Publisher Link]

[6] Afshin Firouzi, Amirmasoud Taki, and Saeed Mohammadzadeh, "Time-Dependent Reliability Analysis of RC Beams Shear and Flexural Strengthened with CFRP Subjected to Harsh Environmental Deteriorations," *Engineering Structures*, vol. 196, 2019. [CrossRef] [Google Scholar] [Publisher Link]

[7] Mohsen Ghabdian et al., "Reliability of Reinforced Concrete Beams in Serviceability Limit State via Microprestress-Solidification Theory, A Structural Health Monitoring Strategy," *Proceedings of the Institution of Mechanical Engineers, Part L: Journal of Materials: Design and Applications*, vol. 236, no. 5, 2022. [CrossRef] [Google Scholar] [Publisher Link]

[8] R. Ian Gilbert, and Robert F. Warner, "Tension Stiffening in Reinforced Concrete Slabs," *Journal of Structural Division, ASCE*, vol. 104, no. 12, pp. 1885-1900, 1978. [CrossRef] [Google Scholar] [Publisher Link]

[9] Marin Grubišić, Jelena Ivošević, and Ante Grubišić, "Reliability Analysis of Reinforced Concrete Frame by Finite Element Method with Implicit Limit State Functions," *Buildings*, vol. 9, no. 5, pp. 1-22, 2019. [CrossRef] [Google Scholar] [Publisher Link]

[10] Bingcheng Guo et al., "Advanced Analytical Model and Reliability Analysis for Long-Term Deflection of FRP Reinforced Concrete Beams with Compression Yielding Mechanism," *Structures*, vol. 80, pp. 1-11, 2025. [CrossRef] [Google Scholar] [Publisher Link]
[11] Abraham M. Hasofer, and Niels C. Lind, "Exact and Invariant Second-Moment Code Format," *Journal of the Engineering Mechanics Division*, vol. 100, no. 1, pp. 111-121, 1974. [CrossRef] [Google Scholar] [Publisher Link]
[12] Rami A. Hawileh, Haya H. Mhanna, and Jamal A. Abdalla, "Effect of Flange Geometry on the Shear Capacity of RC T-Beams," *Procedia Structural Integrity*, vol. 42, pp. 1198-1205, 2022. [CrossRef] [Google Scholar] [Publisher Link]
[13] *IS 456:2000, Plain and Reinforced Concrete — Code of Practice*, 4th Revision, Bureau of Indian Standards, New Delhi, India, 2000. [Google Scholar] [Publisher Link]
[14] Joanna Kaliszuk, "Hybrid Monte Carlo Method in the Reliability Analysis of Structures," *Computer Assisted Mechanics and Engineering Sciences*, vol. 18, pp. 205-216, 2011. [Google Scholar] [Publisher Link]
[15] Niels C. Lind, "Consistent Partial Safety Factors," *Journal of Structural Division, ASCE*, vol. 97, no. 6, pp. 1651-1669, 1971. [CrossRef] [Google Scholar] [Publisher Link]
[16] Mohammed S. Al-Ansari, "Reliability and Flexural Behavior of Triangular and T-Reinforced Concrete Beams," *International Journal of Advanced Structural Engineering*, vol. 7, pp. 377-386, 2015. [CrossRef] [Google Scholar] [Publisher Link]
[17] Osama Ali, "*Time-Dependent Reliability of FRP Strengthened Reinforced Concrete Beams Under Coupled Corrosion and Changing Loading Effects*," Ph.D Thesis, University of Angers, pp. 1-363, 2014. [Google Scholar] [Publisher Link]
[18] Ravindra P. Patil, and K. Manjunath, "An Empirical Expression for Reliability Index of Flanged RC Beams in Limit State of Deflection," *International Journal of Performability Engineering*, vol. 6, no. 4, pp. 373-380, 2010. [CrossRef] [Google Scholar] [Publisher Link]
[19] Ravindra P. Patil, and K. Manjunath, "Time Dependent Performance Analysis of Flanged RC Beam in Limit State of Deflection," *International Journal of Performability Engineering*, vol. 7, no. 4, pp. 379-386, 2011. [CrossRef] [Google Scholar] [Publisher Link]
[20] David Pustka et al., "Probabilistic Reliability Analysis of High-Performance Reinforced Concrete Beam using MATLAB Software," *International Journal of Mechanics*, vol. 8, pp. 101-111, 2014. [Google Scholar] [Publisher Link]
[21] Y.K. Wen, "Reliability and Performance-Based Design," *Structural Safety*, vol. 23, no. 4, pp. 407-428, 2001. [CrossRef] [Google Scholar] [Publisher Link]
[22] JCSS Probabilistic Model Code (PMC), Joint Committee on Structural Safety, 2000. [Online]. Available: https://www.jcss-lc.org/jcss-probabilistic-model-code/